

See discussions, stats, and author profiles for this publication at: <https://www.researchgate.net/publication/6212622>

SO₂ Retention by Reactivated CaO-Based Sorbent from Multiple CO₂ Capture Cycles

ARTICLE *in* ENVIRONMENTAL SCIENCE AND TECHNOLOGY · JULY 2007

Impact Factor: 5.33 · DOI: 10.1021/es0629458 · Source: PubMed

CITATIONS

43

READS

20

2 AUTHORS:



Vasilije Manovic

Cranfield University

92 PUBLICATIONS 1,983 CITATIONS

[SEE PROFILE](#)



Edward Anthony

Cranfield University

261 PUBLICATIONS 7,190 CITATIONS

[SEE PROFILE](#)

SO₂ Retention by Reactivated CaO-Based Sorbent from Multiple CO₂ Capture Cycles

VASILIJE MANOVIC AND EDWARD J. ANTHONY*

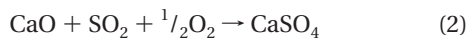
CANMET Energy Technology Centre-Ottawa,
Natural Resources Canada, 1 Haanel Drive, Ottawa,
Ontario, Canada K1A 1M1

This paper examines the reactivation of spent sorbent, produced from multiple CO₂ capture cycles, for use in SO₂ capture. CaO-based sorbent samples were obtained from Kelly Rock limestone using three particle size ranges, each containing different impurities levels. Using a thermogravimetric analyzer (TGA), the sulfation behavior of partially sulfated and unsulfated samples obtained after multiple calcination–carbonation cycles in a tube furnace (TF), following steam reactivation in a pressurized reactor, is examined. In addition, samples calcined/sintered under different conditions after hydration are also examined. The results show that suitably treated spent sorbent has better sulfation characteristics than that of the original sorbent. Thus for example, after 2 h sulfation, >80% of the CaO was sulfated. In addition, the sorbent showed significant activity even after 4 h when >95% CaO was sulfated. The results were confirmed by X-ray diffraction (XRD) analysis, which showed that, by the end of the sulfation process, samples contained CaSO₄ with only traces of unreacted CaO. The superior behavior of spent reactivated sorbent appears to be due to swelling of the sorbent particles during steam hydration. This enables the development of a more suitable pore surface area and pore volume distribution for sulfation, and this has been confirmed by N₂ adsorption–desorption isotherms and the Barrett–Joyner–Halenda (BJH) method. The surface area morphology of sorbent after reactivation was examined by scanning electron microscopy (SEM). Ca(OH)₂ crystals were seen, which displayed their regular shape, and their elemental composition was confirmed by energy-dispersive X-ray (EDX) analysis. The improved characteristics of spent reactivated sorbent in comparison to the original and to the sorbent calcined under different conditions and hydrated indicate the beneficial effect of CO₂ cycles on sorbent reactivation and subsequent sulfation. These results allow us to propose a new process for the use of CaO-based sorbent in fluidized bed combustion (FBC) systems, which incorporates CO₂ capture, sorbent reactivation, and SO₂ retention.

Introduction

Calcium-based sorbents (limestone and dolomite) are typically used for SO₂ capture in fluidized bed combustion (FBC)

systems (1). The global reaction scheme involves calcination (1) and sulfation (2):



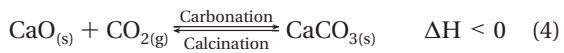
Sulfation is a heterogeneous solid–gas reaction with the formation product (CaSO₄) produced at the reacting surface. The product layer obstructs and restricts contact of CaO and SO₂, and more importantly, fills and blocks sorbent pores as the molar volume of CaCO₃, CaO, and CaSO₄ are, respectively, 37, 17, and 46 cm³/mol. As a result, utilization of CaO is relatively low, usually <45%. This requires the use of extra sorbent above that required by reaction stoichiometry. In industrial combustors, Ca/S molar ratios of 2–2.5 are typical for 90% SO₂ capture. The extra sorbent is, in effect, ballast, which reduces the economic advantages of FBC combustion technology (1, 2). FBC ash from the combustion of high-sulfur fuel typically contains high levels of unreacted calcium oxide, which causes highly exothermic reactions when in contact with water, creating a possible safety hazard. It produces a high-pH leachate when landfilled and, furthermore, is able to react to cause expansion in the landfill, thus increasing the amount of leachate to be treated. The extra limestone used and transported, and disposal of FBC ash, represent additional costs for the technology and can even cause an effective several percent increase in the CO₂ production when firing a high-sulfur fuel such as petroleum coke.

There are numerous possible methods to improve sorbent utilization to obtain a higher final S/Ca molar ratio in the ash. The most thoroughly investigated is hydration by steam (3–7) or liquid water (8, 9), which may be enhanced by grinding (10), sonication (11), and possibly improved via carbonation (12). The basic reaction during partially sulfated sorbent hydration is as follows:



Hydrated sorbents usually (but not always) have a significant ability to react with extra SO₂ and can be reinjected into the combustor for additional sulfur capture. Hydration of fresh calcined limestone may also be used as a method for preparation of sorbent with high reactivity (13, 14).

Recent research (15–18) suggests that Ca-based sorbents may be used for CO₂ capture. The proposed process is based on the following reversible chemical reaction:



CO₂ separation is thus possible in a multicycle process in a dual reactor via reaction of CaO with CO₂ from flue gas in a carbonator and regeneration of sorbent in a calciner (18). However, the reversibility of reaction 4 is limited by sintering, which causes rapid loss of sorbent activity (15–17). This means that the practical use of the carbonation–calcination cycle for CO₂ capture is strongly dependent on the behavior of the spent sorbent during multiple cycles.

In our recent work (19), steam reactivation was investigated. Thermogravimetric analysis (TGA) tests on multicycle carbonation of reactivated sorbent demonstrated better behavior for the reactivated sorbent in comparison to that of the fresh sorbent. The final outcome of these results suggests the practically indefinite use of the sorbent in CO₂ looping cycles in the absence of mechanical loss of material

* Corresponding author phone: (613)996-2868; fax: (613)992-9335; e-mail: banthon@nrcan.gc.ca.

via fragmentation and attrition. However, attrition phenomena may be expected in FBC systems, leading to higher sorbent loss (20). This will be especially important in the case of sorbent hydration because of the reduced hardness of $\text{Ca}(\text{OH})_2$ in comparison to that of CaO/CaCO_3 . A potential approach may be to use the reactivated sorbent for SO_2 retention, which is examined here. Previous results on the use of reactivated sorbent for CO_2 capture (19) and earlier literature on sulfation (21, 22) and carbonation (23, 24) concerning pore filling and product layer diffusion limitations suggested an exploration of the sulfation of such reactivated sorbent for SO_2 retention in FBC systems, since there is clear evidence that sulfation itself can reduce the ability of a sorbent to function in multiple calcination/carbonation cycles with a high degree of reversibility. This will be discussed later.

Materials and Methods

Kelly Rock calcitic limestone is the commercial sorbent used for SO_2 retention in the 165 MWe circulating FBC boiler at Point Aconi, Nova Scotia, Canada. This sorbent has been extensively investigated for use in sulfation, multicycle carbonation, and spent sorbent reactivation (6, 8–12, 16, 19). Here, three particle size fractions ($75\text{--}150\ \mu\text{m}$, $300\text{--}425\ \mu\text{m}$, and $600\text{--}750\ \mu\text{m}$) were examined for SO_2 retention after the spent/sintered sorbent was reactivated following its use in multiple CO_2 capture cycles.

Production of Spent/Sintered Sorbents. A tube furnace (TF) was used to produce sorbents over a wide range of conditions with regard to particle size, sintering and sulfation (19). Calcined/sintered sorbents were obtained at $850\ ^\circ\text{C}$ (2 and 24 h) and $1100\ ^\circ\text{C}$ (24 h) under a N_2 atmosphere. Two types of spent sorbent from CO_2 looping cycles were produced: partially sulfated and unsulfated. Sulfation was performed with sorbents calcined at $850\ ^\circ\text{C}$, using synthetic flue gas (15% CO_2 , 3% O_2 , 1% SO_2 , and N_2 as balance) for 2 h. The partially sulfated samples were then carbonated using a gas mixture containing 20% CO_2 (N_2 balance) for 30 min. Calcination ($850\ ^\circ\text{C}$, 30 min) and carbonation ($650\ ^\circ\text{C}$, 30 min) were performed 20 times. Unsulfated spent sorbent from CO_2 looping cycles was produced in the same way, but without sulfation.

Sorbent Reactivation. The samples of both calcined/sintered and spent sorbent (partially sulfated and unsulfated) obtained from the tube furnace were hydrated in a 2 L Parr 4522M pressure reactor (25). Each sample was placed on a filter paper in an aluminum sample dish within the vapor space of the pressurized reactor. The temperature in the vapor space (which contained saturated steam) was $200\ ^\circ\text{C}$. Air contained in the bomb was purged from the system after the temperature in the bomb exceeded $100\ ^\circ\text{C}$. Hydration duration was 30 min after the temperature in the reactor achieved $200\ ^\circ\text{C}$. When the hydration process was complete, the sample was transferred to a vacuum oven and dried at $50\ ^\circ\text{C}$ for 2 h, which effectively removed all the free water from the samples, as confirmed by TGA analysis. To minimize mass loss, possible change of particle size or morphology, and free water in the sample, the sample was not washed before drying. Sample mass before hydration was typically $\sim 0.5\ \text{g}$, and the samples were weighed after drying. Samples from two repetitions of the hydration process were merged. Sample volumes before and after hydration were measured to provide data on sample swelling due to hydration, and the samples themselves were kept in small, capped jars for subsequent experiments. In this way, their atmospheric exposure was reduced, minimizing possible reaction with atmospheric moisture and CO_2 .

Sulfation. A Perkin-Elmer TGA-7 thermogravimetric analyzer was used for the sulfation experiments. The sample was suspended in a quartz tube (i.d. 20 mm) on a platinum pan (i.d. 5 mm). The temperature and gas used were

controlled by Pyris software. The temperature program included heating to $850\ ^\circ\text{C}$ ($30\ ^\circ\text{C}/\text{min}$) and then keeping the temperature at that level for 260 min. The program started with the introduction of N_2 , which was replaced with gas mixture: synthetic flue gas (15% CO_2 , 3% O_2 , 2250 ppm SO_2 and N_2 balance) 10 min after the temperature reached $850\ ^\circ\text{C}$. Sulfation was performed for 240 min. For the last 10 min, N_2 (gas mixture replaced with N_2) was introduced to check the thermal stability of the product obtained; i.e., to confirm that the observed mass increase was due only to CaSO_4 formation (and not, for example, because of sulfide formation). Mass loss during the last 10 min in all runs was negligible. The gas flow rate during runs was controlled by flowmeter and was $40\ \text{cm}^3/\text{min}$. The sorbent masses were chosen so that the mass of CaO in the samples was approximately the same, $\sim 10\ \text{mg}$, so that the rate of S/Ca molar ratio increase during experiments was $1.35/\text{h}$. Hydration, carbonation and sulfation levels were calculated on the basis of the TGA data.

Sample Characterization. Chemical compositions based on X-ray fluorescence (XRF) elemental analyses for the original particle size fractions have been given elsewhere (19). Identification of compounds and their content in hydrated samples before and after additional sulfation were obtained by X-ray diffraction (XRD). The morphologies of sample surface areas were examined by scanning electron microscopy (SEM) using a Hitachi S3400 microscope with $20\ \text{kV}$ of accelerating voltage. SEM images of samples were obtained at different magnifications, starting from $20\times$ to $10\,000\times$. The microscope was equipped with energy-dispersive X-ray (EDX) analyzers, which enabled us to examine elemental composition of sample surfaces. Changes in pore surface area and volume distribution were obtained using data on nitrogen adsorption/desorption and the Barrett–Joyner–Halenda (BJH) model.

Results and Discussion

The most significant results of this study are summarized in Table 1. As expected, sulfation of natural sorbent is substantially incomplete. The values of the S/Ca molar ratio in the tube furnace were $\leq 30\%$. Higher values were obtained in the TGA, presumably because of easier interparticle mass transfer in the TGA, i.e., because of the smaller sample mass ($\sim 20\ \text{mg}$ in the TGA vs $\sim 1\ \text{g}$ in the TF). Maximum sulfation was obtained for the $75\text{--}150\ \mu\text{m}$ sample in TGA runs (33.61% for 2 h and 37.16% for 4 h). In the tube furnace, S/Ca molar ratio increased from 26.99% ($600\text{--}750\ \mu\text{m}$) to 30.55% ($75\text{--}150\ \mu\text{m}$) as expected since sulfation increases with decreasing particle size. The original values of S/Ca molar ratio $<1\%$ are because a small amount of sulfur is present in the original samples.

Table 1 gives the V_2/V_1 volume ratio, which represents the ratio of sample volumes after and before steam hydration. The V_2/V_1 values for samples used in CO_2 looping cycles are, in general, higher in the case of unsulfated samples. With increasing particle size, the V_2/V_1 values increase and this is more noticeable in the case of sulfated samples, i.e., V_2/V_1 decreases with increasing level of sample sulfation. The V_2/V_1 values are high as a result of higher molar volume of $\text{Ca}(\text{OH})_2$ in comparison to the molar volume of CaO ($33\ \text{cm}^3/\text{mol}$ vs $17\ \text{cm}^3/\text{mol}$). This is a very significant result and shows that particles produced during CO_2 cycles swell during steam reactivation to a greater degree than as the result of product molar volume increases. On the other hand, the samples calcined/sintered under different conditions ($1100\ ^\circ\text{C}$ for 24 h and $850\ ^\circ\text{C}$ for 2 and 24 h) have lower V_2/V_1 values, which are not dependent on particle size. This means that CO_2 multicycle treatment has a beneficial effect for steam reactivation, and this may be correlated with cracks on particle surfaces shown by SEM (see below).

TABLE 1. Sample Characteristics before Sulfation in TGA and Sulfation Levels after TGA Runs^a

sample	pretreatment	before TGA sulfation					after TGA sulfation	
		S/Ca (%)	V ₂ /V ₁ (%)	H ₂ O/Ca (%)	C/Ca (%)	Σ/Ca (%)	S/Ca (2 h) (%)	S/Ca (4 h) (%)
KR01 (75–150 μm)	original sample	0.78	n/a	0.00	101.44	102.22	33.61	37.16
KR37 (75–150 μm)	calcination, sulfation,	30.55	~2.4	54.95	10.65	96.15	84.34	91.00
KR38 (300–425 μm)	20 CO ₂ cycles in TF,	28.42	~3.5	54.24	12.15	94.81	89.22	97.13
KR39 (600–750 μm)	hydration	26.99	~4.1	53.42	15.63	96.04	88.66	97.35
KR40 (75–150 μm)	calcination, 20 CO ₂	0.78	~3.8	69.61	28.77	99.16	77.79	93.50
KR41 (300–425 μm)	cycles in TF,	0.33	~4.0	78.09	20.26	98.68	73.98	92.59
KR42 (600–750 μm)	hydration	0.40	~4.2	72.64	24.09	97.13	81.10	97.91
KR43 (75–150 μm)	calcination	0.78	~1.9	84.27	5.92	90.97	65.83	73.84
KR44 (300–425 μm)	(1100 °C, 24 h),	0.33	~2.0	80.78	5.57	86.68	66.26	76.12
KR45 (600–750 μm)	hydration	0.40	~2.1	80.98	3.78	85.16	63.67	73.45
KR46 (75–150 μm)	calcination	0.78	~1.8	84.59	10.27	95.64	74.96	81.37
KR47 (300–425 μm)	(850 °C, 24 h),	0.33	~1.8	88.20	5.81	94.34	66.00	74.22
KR48 (600–750 μm)	hydration	0.40	~1.8	89.38	6.04	95.82	61.98	74.07
KR49 (75–150 μm)	calcination	0.78	~1.7	86.39	7.29	94.46	74.30	82.91
KR50 (300–425 μm)	(850 °C, 2 h),	0.33	~1.7	87.85	5.81	93.99	66.51	79.23
KR51 (600–750 μm)	hydration	0.40	~1.7	87.16	3.13	90.69	61.25	74.62
KR05-fresh		0.33	n/a	0.00	0.00	0.33	21.80	29.62
KR05-1 day	calcination	0.33	n/a	16.23	0.54	17.10	24.52	32.50
KR05-7 days	(1100 °C, 24 h)	0.33	n/a	80.32	5.59	86.24	52.91	67.63
KR05-35 days		0.33	n/a	61.21	25.49	87.03	56.41	71.25
KR44-fresh	calcination	0.33	n.d.	82.21	4.19	86.73	58.70	71.55
KR44-1 day	(1100 °C, 24 h),	0.33	n.d.	78.59	10.63	89.55	63.63	77.68
KR44-7 days	hydration	0.33	n.d.	73.93	16.20	90.46	66.97	80.94
KR44-35 days		0.33	n.d.	65.29	28.15	93.77	63.21	77.34

^a Notation: S/Ca—sulfation—the molar ratio S/Ca × 100% (2 and 4 h are durations of sulfation in TGA); H₂O/Ca—hydration—the molar ratio H₂O/Ca × 100% (only H₂O in Ca(OH)₂); C/Ca—carbonation—the molar ratio C/Ca × 100%; Σ/Ca—total molar ratio S/Ca + H₂O/Ca + C/Ca; V₂/V₁—ratio of sample volumes after/before hydration.

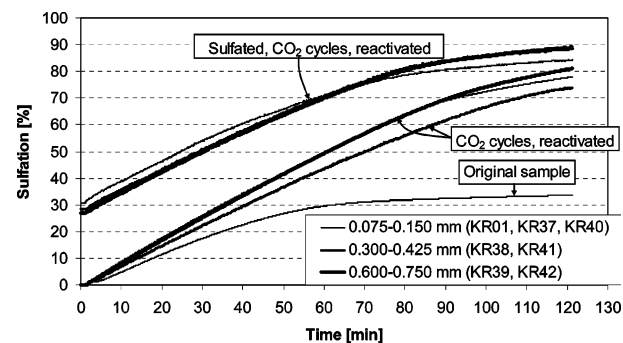
TABLE 2. Quantitative XRD Analyses of Sulfated Sample Spent in 20 CO₂ Cycles and Hydrated by Steam (KR38); Sulfated Sample Spent in 20 CO₂ Cycles, Hydrated by Steam and Sulfated in TGA (KR38S); and Unsulfated Sample Spent in 20 CO₂ Cycles, Hydrated by Steam and Sulfated in TGA (KR41S)

component	KR38	KR38S	KR41S
CaSO ₄	49.2 wt %	97.6 wt %	94.7 wt %
CaCO ₃	16.9 wt %	n/a	n/a
Ca(OH) ₂	32.8 wt %	n/a	n/a
CaO	n.d.	0.7 wt %	1.3 wt %
SiO ₂	1.0 wt %	1.8 wt %	4.0 wt %

Swelling of sorbent particles during steam hydration and consequent increase in sample volume lead one to expect a higher level of sulfation of the reactivated sample. Namely, given the molar volume ratio CaSO₄/CaO is (46 cm³/mol)/(17 cm³/mol) = 2.7, increased V₂/V₁ values obtained for spent and reactivated sorbent samples are likely to allow continuous sulfation unlimited by pore filling due to the bulky sulfation product.

The TGA sulfation of reactivated samples confirms the assumption of their high activity. Sulfation levels after 2 h reached ~80%. Moreover, the samples after 80% sulfation showed a relatively high sulfation rate during a further 2 h of sulfation. The final results represent almost total sulfation (~95%), calculated on the basis of the TGA data for sulfated samples. Some lower values of sulfation are obtained for samples calcined/sintered at higher temperatures and longer durations, especially at 1100 °C/24 h. This showed that CO₂ looping cycles had a beneficial effect on hydration and subsequent sulfation behavior of these samples.

The results for quantitative XRD analyses for the reactivated sample KR38 and the samples obtained after TGA sulfation of reactivated samples KR38 and KR41 (KR38S and

**FIGURE 1. TGA sulfation runs for original and reactivated sorbent samples. Note: the curves KR38 and KR39, and KR40 and KR42 are overlapped for the most part.**

KR41S) are given in Table 2. The corresponding XRD spectra can be seen in the Supporting Information (Figure S1). XRD analyses also clearly confirm high sulfation of reactivated samples. The samples KR38S and KR41S are primarily calcium sulfate with traces of calcium oxide and quartz. CaO contents in the sample after reactivation were below detection limits, which indicate total hydration of samples and in agreement with the data in Table 1 (values Σ/Ca). Also, XRD of the samples showed high crystallinity, with no amorphous phase being detected.

The kinetics during the first 2 h sulfation of the spent samples, reactivated by steam, can be seen from Figure 1. In the same figure, for comparison, the sulfation curve for the original sorbent is also given. It can be seen that there are major differences between sulfation of the original and reactivated samples. Sulfation of CaO is limited by diffusion through the product layer (CaSO₄), which forms an outer shell and hinders contact of reactants (CaO and SO₂) (21, 22), and hence, sulfation curves for CaO produced from limestone have a typical shape as shown in Figure 1 for the

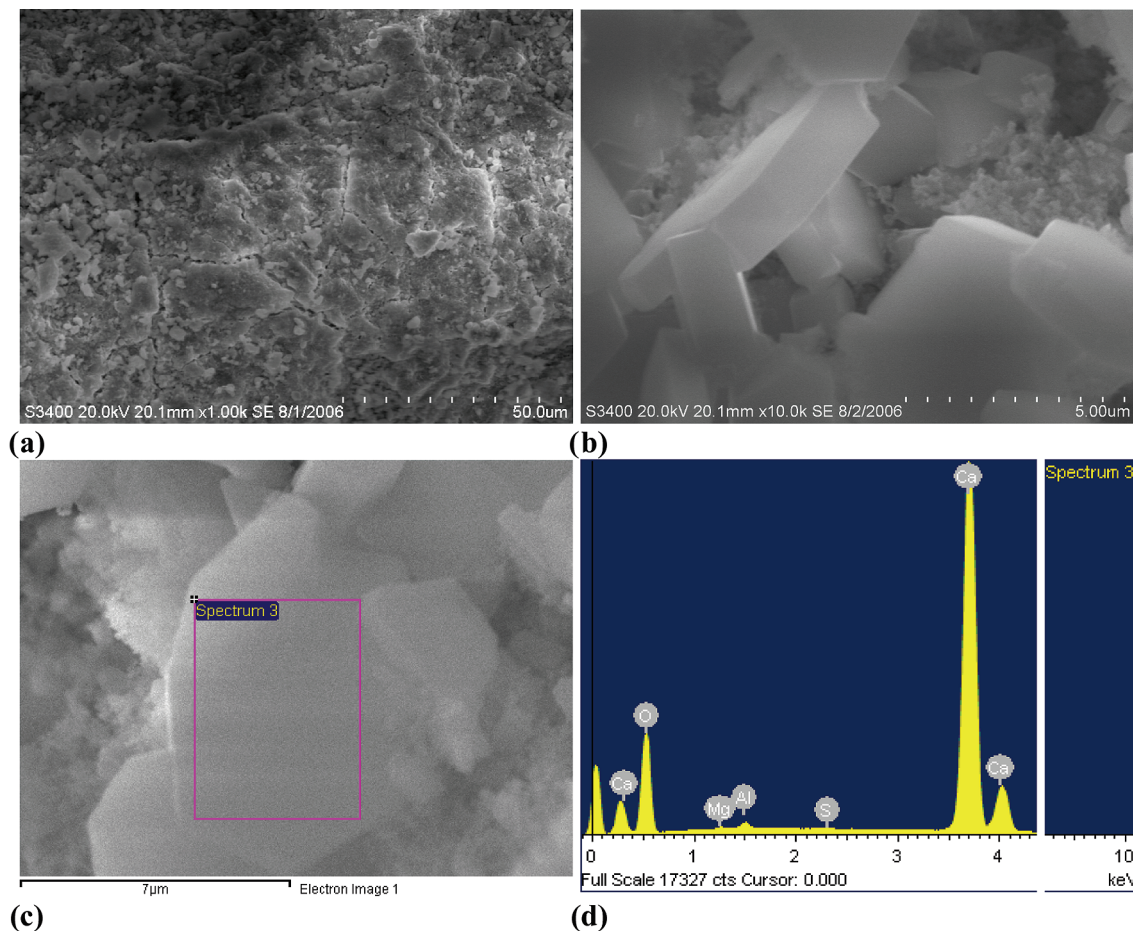


FIGURE 2. SEM images of sorbent surface area (a) after 20 CO_2 cycles, (b) and (c) after hydration, and (d) EDX spectrum of single crystal (in c) formed after hydration.

original sample KR01. The sulfation had an initial faster stage, and after 60 min, 30% sulfation was achieved. After this stage, sulfation becomes very slow because of diffusion limitations. During the next 60 min, only a few percent of additional sulfation occurs.

The shapes of sulfation curves for the reactivated sorbent are very different. The beginning stage is faster in comparison to that for the original sorbent as there is greater surface area available for reaction for the reactivated sorbent (see below). The shift to the slower stage is not clearly apparent, but occurs later (about 80–90 min) and corresponds to a higher level of sulfation than for the original sorbent. Furthermore, the sulfation rate is not reduced so drastically and during the next 30 min the sulfation level increases by an additional ~10%. Final values, after 4 h are >90% (Table 1), which has also been confirmed by XRD (Table 2, Figure S1).

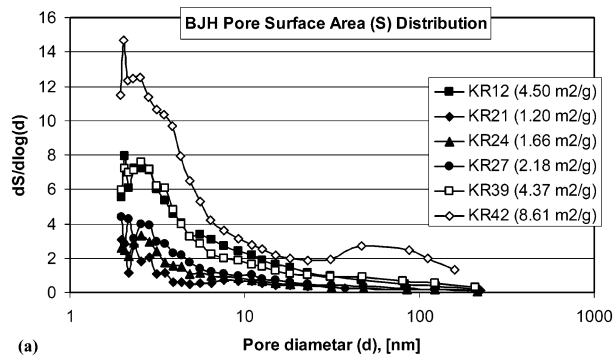
The kinetics of sulfation of sorbent samples calcined/sintered at different temperatures and times are similar to those of the reactivated spent sorbent. The corresponding charts can be seen in Figure S2 (Supporting Information). However, this type of reactivated sorbent exhibits inferior performance, with final sulfation levels $\leq 80\%$, which is lower than the values obtained for sorbent from CO_2 multicycles. Lower sulfation levels were obtained for a sample sintered at 1100 °C for 24 h. This is in agreement with the Σ/Ca ($\text{S}/\text{Ca} + \text{H}_2\text{O}/\text{Ca} + \text{C}/\text{Ca}$) values. From Table 1 it can be seen that minimal values (85.16–90.97%) of Σ/Ca are produced for “deeply” sintered samples. The maximal Σ/Ca values are obtained for unsulfated samples after CO_2 cycles, which means the best reactivation is achieved for these samples.

A possible explanation for the enhanced behavior in hydration and sulfation of sorbents treated with CO_2 may be

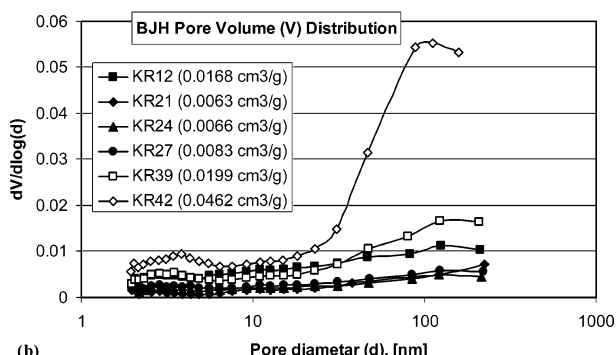
the cracks detected at the particle surface by SEM, (see Figure 2a). These cracks simplify penetration of steam into the particle interior resulting in better hydration and particle swelling, which subsequently enhances the degree of sulfation finally produced.

An interesting observation from the experimental work was that these samples showed considerable reactivity with atmospheric moisture and CO_2 . Hydrated samples contained more CO_2 than those not hydrated. Also, during handling, it was noticed that samples rapidly absorbed H_2O and CO_2 ($\text{H}_2\text{O}/\text{Ca}$ and C/Ca ratios), which affected sulfation. To evaluate the degree of change and influence on sulfation, two samples were analyzed following different preparation times. A $300\text{--}425\text{ }\mu\text{m}$ sample was sintered at 1100 °C for 24 h. One part of the obtained sample was sulfated in the TGA immediately after sintering (KR05-fresh) and after 1, 7, and 35 days. Another part of the sample was hydrated and sulfated (fresh, 1, 7, and 35 days). Over a period of 35 days these samples were left in uncovered containers.

The results in Table 1 show fast hydration of the sintered sample; the $\text{H}_2\text{O}/\text{Ca}$ after 24 h was 16.23%, and after 7 days 80.32%. By 35 days, the water content decreased due to carbonation with CO_2 from the air, resulting in 25.49% of the sample being carbonated. Interestingly, these samples also showed enhanced sulfation behavior, with a sulfation level reaching 71.25%. However, this was not explored further given that this work is focused on the effects of sintering on the reactivity of sorbents. For the hydrated sample (KR44), hydration decreased from 82.21 to 65.29% because of sample carbonation (4.19–28.15%). The Σ/Ca molar ratio regularly increased to 93.77%. The TGA sulfation curves are given in the Supporting Information, Figure S3.



(a)



(b)

FIGURE 3. Pore surface area (a) and pore volume (b) distribution of investigated sorbent (600–750 μm): original calcined sorbent (KR12); partially sulfated (KR21); partially sulfated and 20 CO_2 cycles (KR24); unsulfated after 20 CO_2 cycles (KR27); partially sulfated, 20 CO_2 cycles, hydrated and calcined (KR39); unsulfated, 20 CO_2 cycles, hydrated and calcined (KR42). The values in brackets in diagrams are cumulative BJH values of pore surface area and pore volume.

The SEM analyses of surface area morphologies after spent sample hydration showed the appearance of crystals with very regular surface areas (Figure 2b and c). Elemental compositions of these crystals were analyzed by EDX spectrometry. The EDX spectrum in Figure 2d shows that O and Ca peaks predominate, with Mg, Al, and S present in trace amounts. This is evidence that the main component in the crystals is $\text{Ca}(\text{OH})_2$. Moreover, it was found that S is concentrated in some parts of the sample area, but not as part of the regular crystal structure. This indicates that, during steam reactivation of sorbent spent in CO_2 capture cycles, recrystallization occurs. The recrystallization enables the formation of $\text{Ca}(\text{OH})_2$ in the form of separate crystals. Subsequent calcination of reactivated samples gives separated crystals of CaO, which are not surrounded by CaSO_4 and are, hence, more active for sulfation in comparison to the partially sulfated and spent CaO present before reactivation.

The specific pore surface area and pore volume distribution of sorbents were determined using the N_2 adsorption/desorption data and the BJH method. The results of analyses are presented in Figure 3. As expected the main contribution to pore surface area (Figure 3a) is from small pores (2–3 nm), and with increasing pore diameter, the contribution decreases. Moreover, with sintering, a large number of small pores are eliminated, which results in a decrease in total pore surface area. This can be seen from the drop of pore surface area of sorbent after CO_2 capture cycles (KR27) in comparison with that for the original calcined sorbent (KR12). Partially sulfated sample (KR21) has the least pore surface area because of pore filling by the bulky product (CaSO_4). However, after 20 CO_2 capture cycles, KR24 surface area increases somewhat. The most important conclusion from pore surface area analyses is that there is a significant increase

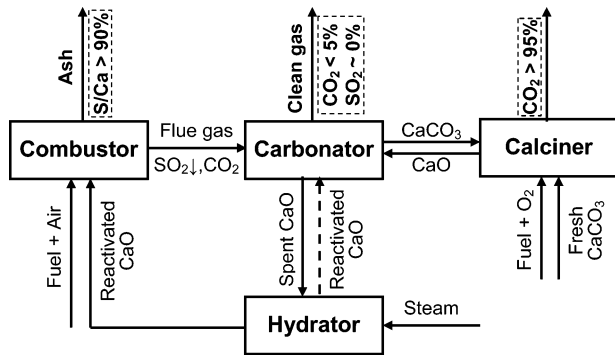


FIGURE 4. Schematic representation of the proposed process, which integrates CO_2 capture and SO_2 retention with sorbent reactivation.

after hydration. The reactivated unsulfated sample (KR42) has a much higher surface area than the original sorbent, and as a result, better behavior during sulfation. It is interesting that this sample has a small peak in pore surface area distribution in the area 50–100 nm. Moreover, the spent, partially sulfated (26.99%) sample after reactivation (KR39) has very close pore surface area distribution to that of the original sample.

Pore volume distribution (Figure 3b) corresponds to the pore surface area distribution, but the contribution to pore volume increases as pore diameter increases. Pore volume of the sorbent after CO_2 capture cycles (KR24 and KR27) and partially sulfated sorbent (KR21) are significantly smaller than in the original calcined sorbent (KR12). This is especially noticeable for small pores (< 6 nm), which are eliminated during sulfation and sintering. Small intraparticle grains disappear and are transferred to neighboring grains, making the large grains even larger. This type of sorbent is practically unusable for sulfation. Pore volume increases after reactivation (KR39 and KR42), but more for larger pores (~100 nm). This is in agreement with the literature (14) that the pore volume is primarily contained in much larger pores in the case of CaO produced from $\text{Ca}(\text{OH})_2$ when compared with CaO produced from CaCO_3 . For large pores, pore volume after reactivation is much higher even than that for the original sorbent. Taking into account the fact that sulfation is mainly limited by pore filling, i.e., diffusion through product layer, increase of pore volume is very favorable. Higher pore volumes of reactivated sorbent are in close agreement with sulfation data (Tables 1 and 2, Figure 1) and the improved performance of reactivated compared to original sorbent.

The superior behavior of sorbent in carbonation (19) and in sulfation, as shown in this work, supports the idea of a new process of utilization of CaO-based sorbents in FBC systems for enhanced CO_2 capture and enhanced SO_2 retention, schematically shown in Figure 4. The TGA test data support the belief that a process can be developed in which the final products are ash with little or no unreacted CaO, clean flue gas with “zero” SO_2 and less than 5% CO_2 , and a separated stream of practically pure CO_2 (>95%). The high S/Ca molar ratio in the ash reduces the problems of ash disposal (and disposal of spent sorbent from CO_2 cycles) and cuts waste solids production by half in terms of the amount of sorbent needed for SO_2 retention. The relationship between the average CaO capture efficiency (the maximum carbonation for any given number of cycles), η_{CO_2} , the C/S molar ratio in fuel and number of cycles (n) is: $n = \eta_{\text{CO}_2} \times \text{C/S}$. The main limitation for this approach in FBC systems may well be sorbent attrition, and it may be worth exploring pelletization concepts to use such solids further.

In the case of sorbents with high C/S molar ratio and/or with greater tendency to sintering (decay reactivity), improved performance may be obtained using the reactivated sorbent

for enhancement of carbonation. An additional advantage of the proposed process is separation of CO₂ capture from SO₂ retention. Recent investigations (19, 26) showed very negative effects of sulfation on carbonation, because the CaSO₄ layer formed impedes diffusion of CO₂ and reaction with CaO. In the proposed scheme, SO₂ retention occurs predominantly in the combustor, with only small concentrations of SO₂ entering the carbonator with the flue gas.

Supporting Information Available

Three figures show the XRD spectra of samples from Table 2, TGA sulfation runs for sorbents obtained under different conditions, and TGA sulfation runs for sorbents exposed to air for different durations. This material is available free of charge via the Internet at <http://pubs.acs.org>.

Literature Cited

- (1) Anthony, E. J.; Granatstein, D. L. Sulfation phenomena in fluidized bed combustion systems. *Prog. Energy Combust. Sci.* **2001**, *27*, 215–236.
- (2) MacKenzie, A.; Granatstein, D. L.; Anthony, E. J. Economic case study of ash reactivation for a generic 150 MWe Canadian circulating fluidized bed combustor. *Int. J. Environ. Stud.* **2007**, in press.
- (3) Laursen, K.; Duo, W.; Grace, J. R.; Lim, J. Sulfation and reactivation characteristics of nine limestones. *Fuel* **2000**, *79*, 153–163.
- (4) Scala, F.; Montagnaro, F.; Salatino, P. Enhancement of sulfur uptake by hydration of spent limestone for fluidized-bed combustion application. *Ind. Eng. Chem. Res.* **2001**, *40*, 2495–2501.
- (5) Davini, P. Properties and reactivity of reactivated calcium-based sorbents. *Fuel* **2002**, *81*, 763–770.
- (6) Wu, Y.; Anthony, E. J.; Jia, L. Steam hydration of CFBC ash and the effect of hydration conditions on reactivation. *Fuel* **2004**, *83*, 1357–1370.
- (7) Gora, D.; Anthony, E. J.; Bulewicz, E. M.; Jia, L. Steam reactivation of 16 bed and fly ashes from industrial-scale coal-fired fluidized bed combustors. *Fuel* **2006**, *85*, 94–106.
- (8) Wu, Y.; Anthony, E. J.; Jia, L. An experimental study on hydration of partially sulfated FBC ash. *Combust. Sci. Technol.* **2002**, *174*, 171–181.
- (9) Wang, J.; Wu, Y.; Anthony, E. J. The hydration behavior of partially sulfated fluidized bed combustor sorbent. *Ind. Eng. Chem. Res.* **2005**, *44*, 8199–8204.
- (10) Anthony, E. J.; MacKenzie, A.; Trass, O.; Gandolfi, E.; Iribarne, A. P.; Iribarne, J. V.; Burwell, S. M. Advanced fluidized bed combustion sorbent reactivation technology. *Ind. Eng. Chem. Res.* **2003**, *42*, 1162–1173.
- (11) Anthony, E. J.; Jia, L.; Cyr, L.; Smith, B.; Burwell, S. The enhancement of hydration of fluidized bed combustion ash by sonication. *Environ. Sci. Technol.* **2002**, *36*, 4447–4453.
- (12) Rao, A.; Anthony, E. J.; Jia, L.; Macchi, A. Carbonation of FBC ash by sonochemical treatment. *Fuel* **2007**, in press.
- (13) Bruce, K. R.; Gullett, B. K.; Beach, L. O. Comparative SO₂ reactivity of CaO derived from CaCO₃ and Ca(OH)₂. *AICHE J.* **1989**, *35*, 37–41.
- (14) Gullett, B. K.; Bruce, K. R. Pore distribution changes of calcium-based sorbents reacting with sulfur dioxide. *AICHE J.* **1987**, *33*, 1719–1726.
- (15) Shimizu, T.; Hirama, T.; Hosoda, H.; Kitano, K.; Inagaki, M.; Tejima, K. A twin fluid-bed reactor for removal of CO₂ from combustion processes. *Trans. IChemE* **1999**, *77* (part A), 62–68.
- (16) Salvador, C.; Lu, D.; Anthony, E. J.; Abanades, J. C. Enhancement of CaO for CO₂ capture in an FBC environment. *Chem. Eng. J.* **2003**, *96*, 187–195.
- (17) Abanades, J. C.; Anthony, E. J.; Alvarez, D.; Lu, D.; Salvador, C. Capture of CO₂ from combustion gases in a fluidized bed of CaO. *AICHE J.* **2004**, *50*, 1614–1622.
- (18) Abanades, J. C.; Anthony, E. J.; Wang, J.; Oakey, A. Fluidized bed combustion systems integrating CO₂ capture with CaO. *Environ. Sci. Technol.* **2005**, *39*, 2861–2866.
- (19) Manovic, V.; Anthony, E. J. Steam reactivation of spent CaO-based sorbent for multiple CO₂ capture cycles. *Environ. Sci. Technol.* **2007**, *41*, 1420–1425.
- (20) Jia, L.; Hughes, R.; Lu, D.; Anthony, E. J.; Lau, I. Attrition of calcining limestones in circulating fluidized bed systems. *Ind. Eng. Chem. Res.* accepted for publication.
- (21) Borgwardt, R. H.; Bruce, K. R.; Blake, J. An investigation of product-layer diffusivity for CaO sulfation. *Ind. Eng. Chem. Res.* **1987**, *26*, 993–998.
- (22) Hsia, C.; St. Pierre, G. R.; Raghunathan, K.; Fan, L.-S. Diffusion through CaSO₄ formed during the reaction of CaO with SO₂ and O₂. *AICHE J.* **1993**, *39*, 698–700.
- (23) Bhatia, S. K.; Perlmutter, D. D. Effect of the product layer on the kinetics of the CO₂-lime reaction. *AICHE J.* **1983**, *29*, 79–86.
- (24) Mess, D.; Sarofim, A. F.; Longwell, J. P. Product layer diffusion during the reaction of calcium oxide with carbon dioxide. *Energy Fuels* **1999**, *13*, 999–1005.
- (25) Anthony, E. J.; Jia, L.; Woods, J.; Roque, W.; Burwell, S. Pacification of high calcic residues using carbon dioxide. *Waste Manage.* **2000**, *20*, 1–13.
- (26) Ryu, H.; Grace, J. R.; Lim, C. J. Simultaneous CO₂/SO₂ capture characteristics of three limestones in a fluidized-bed reactor. *Energy Fuels* **2006**, *20*, 1621–1628.

Received for review December 12, 2006. Revised manuscript received March 22, 2007. Accepted April 4, 2007.

ES0629458